frontiers

Supplementary Material

Novel oxygen optode sensor with fast response time: an in-depth characterization and assessment of the HydroFlash O_2, applicable for several ocean observing platforms

Tobias Hahn* **and Arne Körtzinger**
*Correspondence:
Tobias Hahn
thahn@geomar.de

1 SUPPLEMENTARY FIGURES

1.1 O_2 and temperature dependence and calibration: accuracy and precision

Examples of calibration results for 4330 and HydroFlash O_2 optodes are shown in the following figures.

1.1.1 4330 optodes

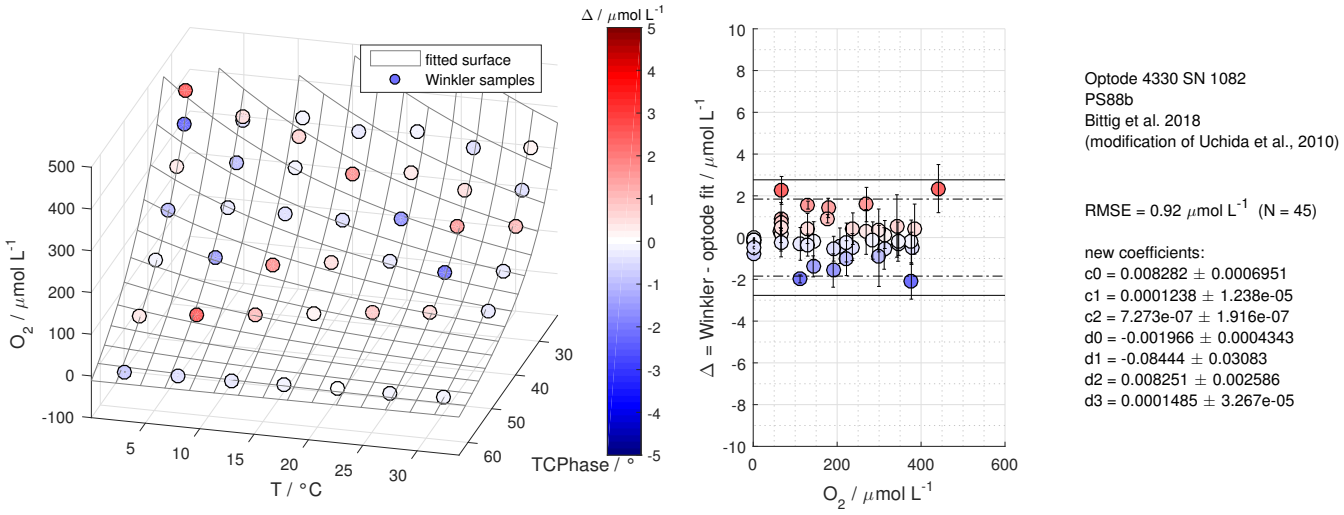

Figure S1: Calibration results of 4330-1082 from multi-point calibration 1

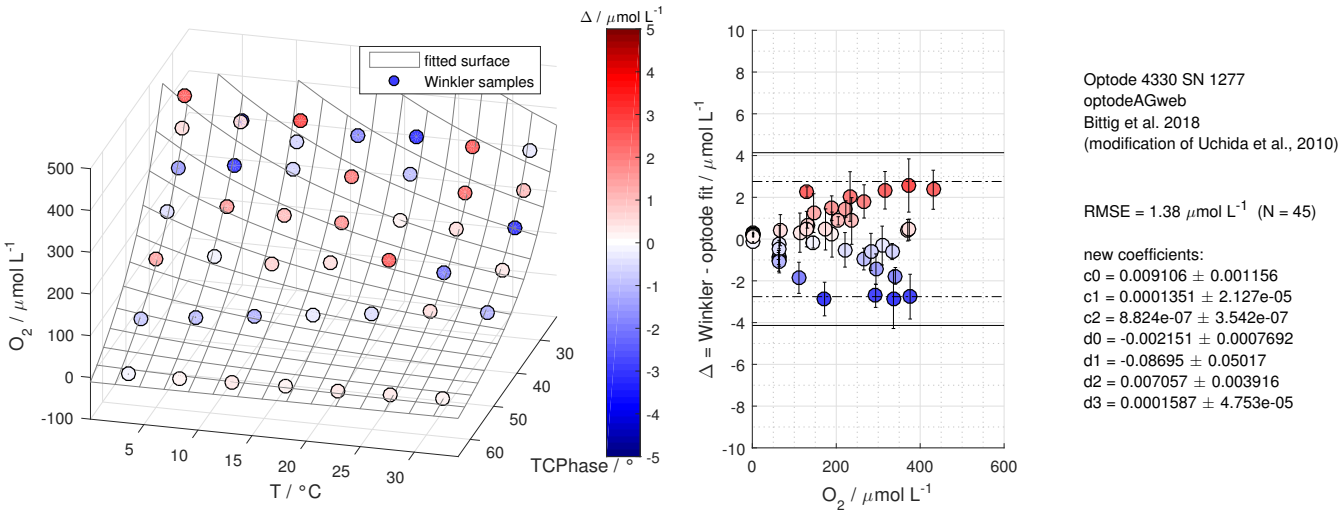

Figure S2: Calibration results of 4330-1277 from multi-point calibration 2

1.1.2 CONTROS HydroFlash® O_2 optodes

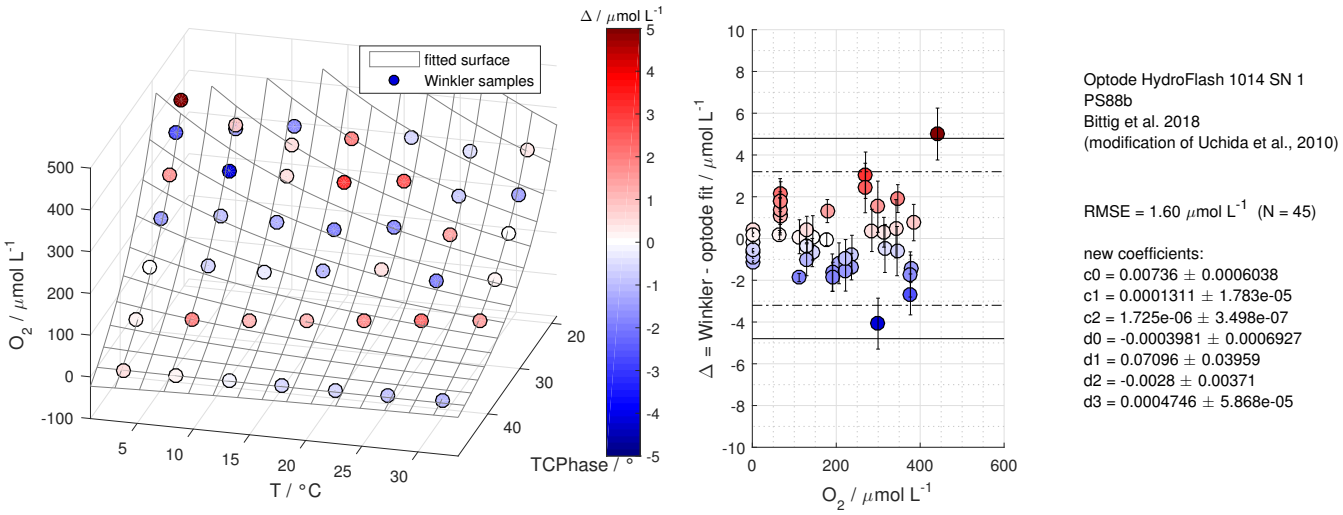

Figure S3: If the 3 × RMSE criterion was exceeded, we considered the calibration results with the respective number of calibration points as invalid (*here*: HF14-01 with n = 45 from multi-point calibration 1).

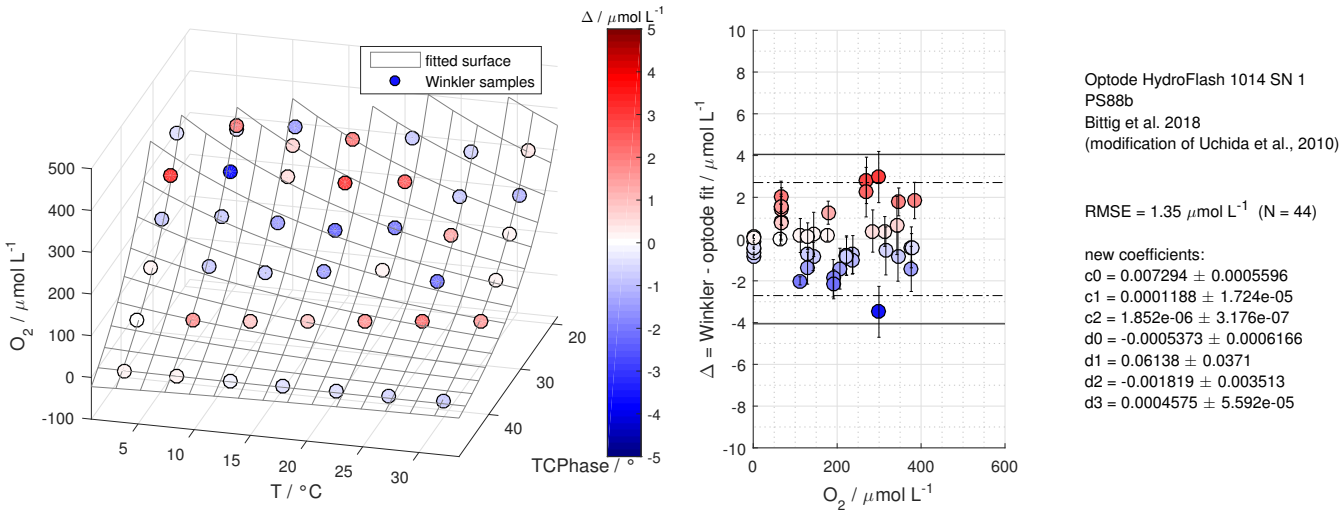

Figure S4: Calibration results of HF14-01 from multi-point calibration 1 without exceeding the 3 x RMSE criterion

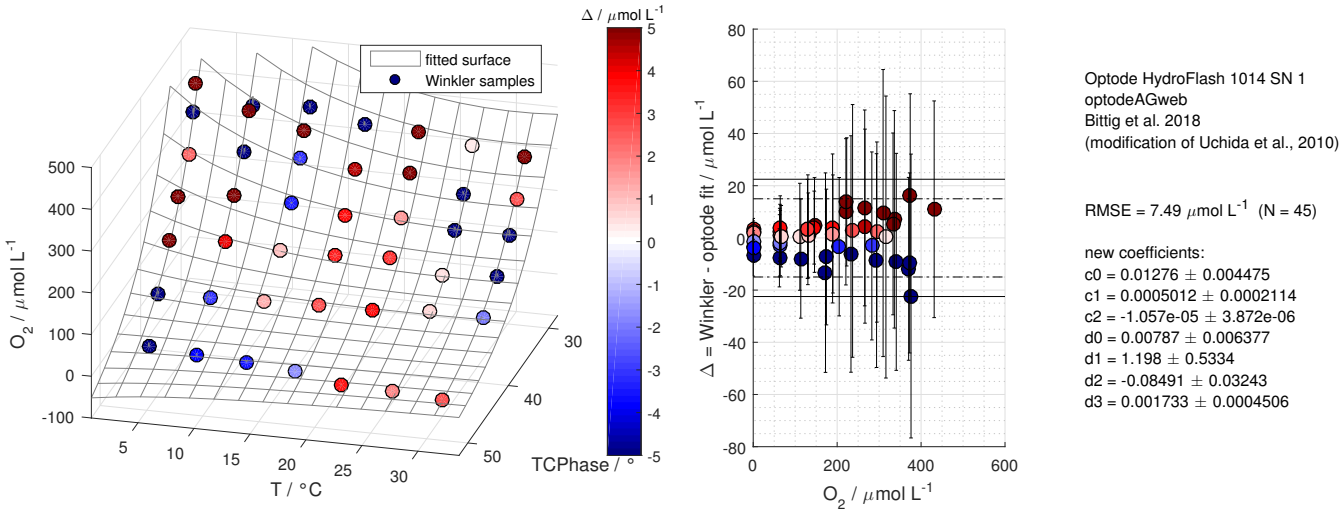

Figure S5: Calibration results of HF14-01 from multi-point calibration 2. This optode's sensor spot was damaged which expressed in much higher misfit and RMSE between the reference and optode.

1.2 0 % and 100 % O_2 calibration: re-adjustments

Exemplary results of HydroFlash O_2 optodes from re-adjustments, which were performed during laboratory and field experiments, are shown in the following figures.

1.2.1 Re-adjustments from laboratory experiments

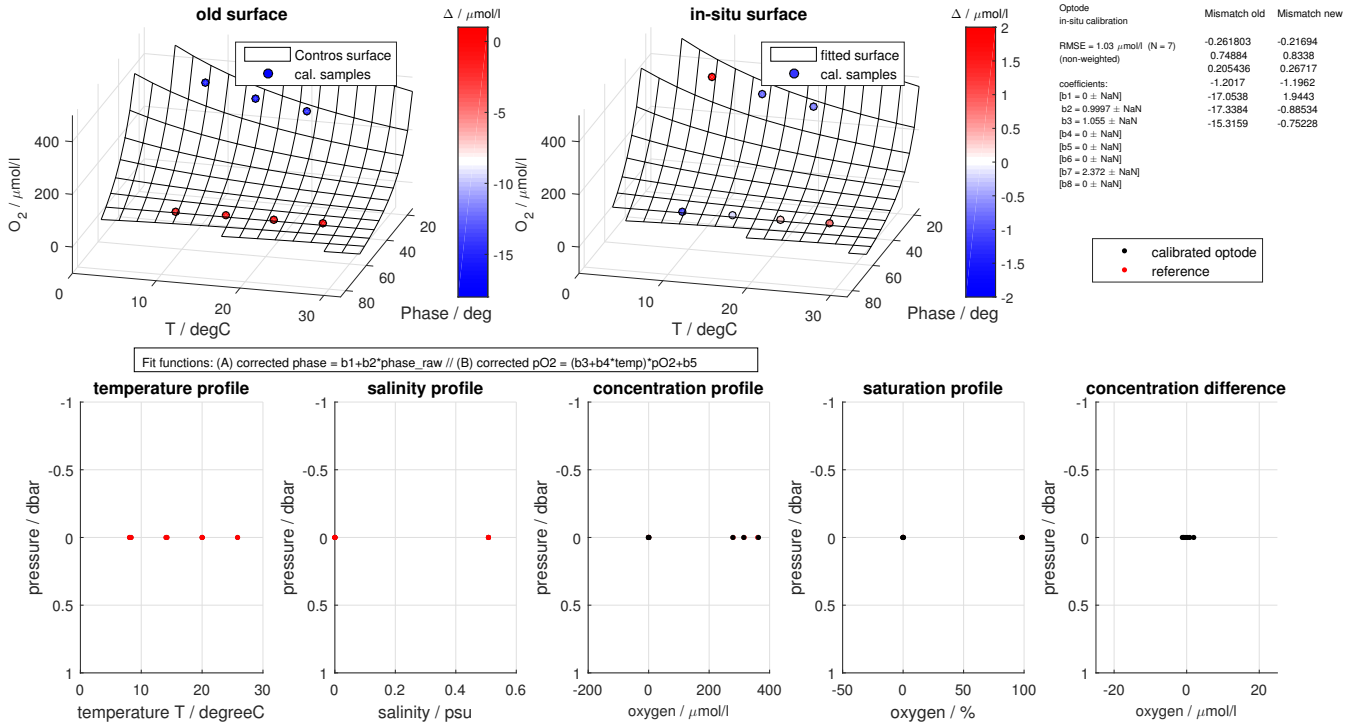

Figure S6: Re-adjustment of HF17-01 from two-point calibration 2 in the laboratory

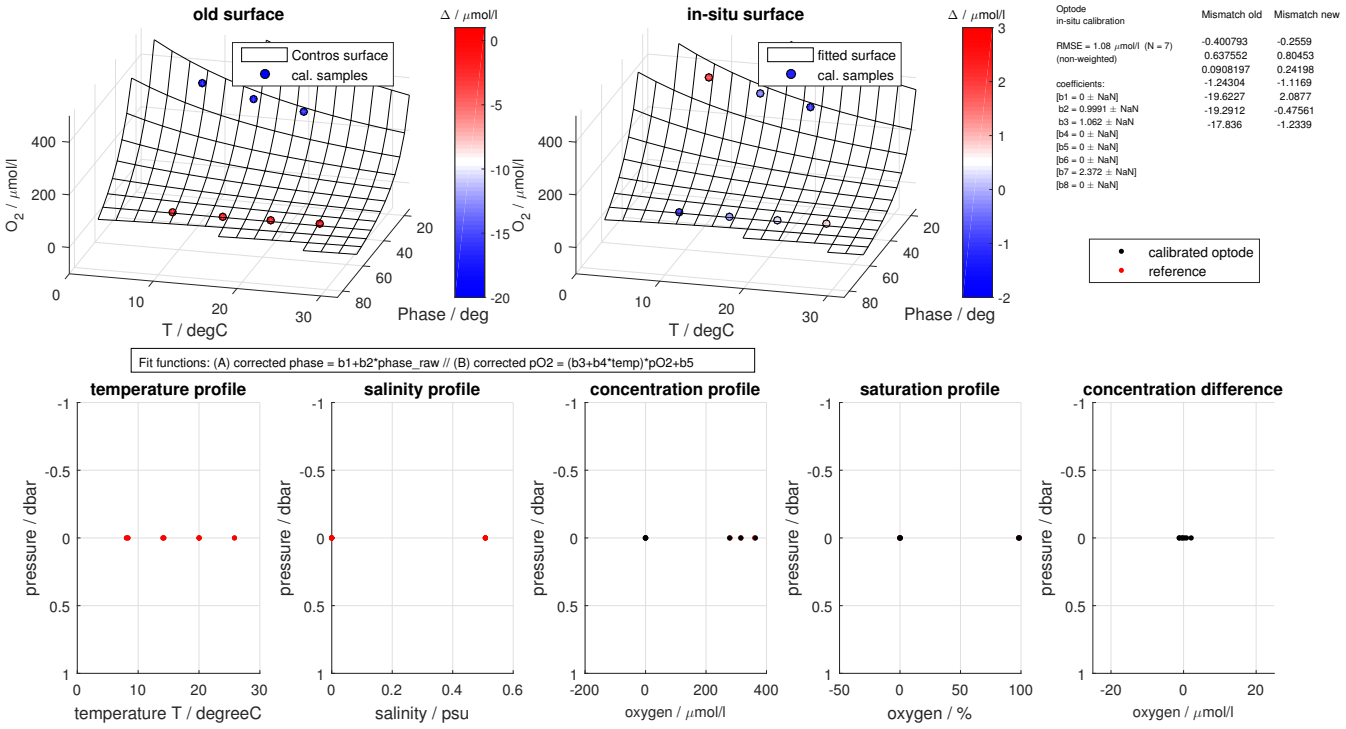

Figure S7: Re-adjustment of HF17-02 from two-point calibration 2 in the laboratory

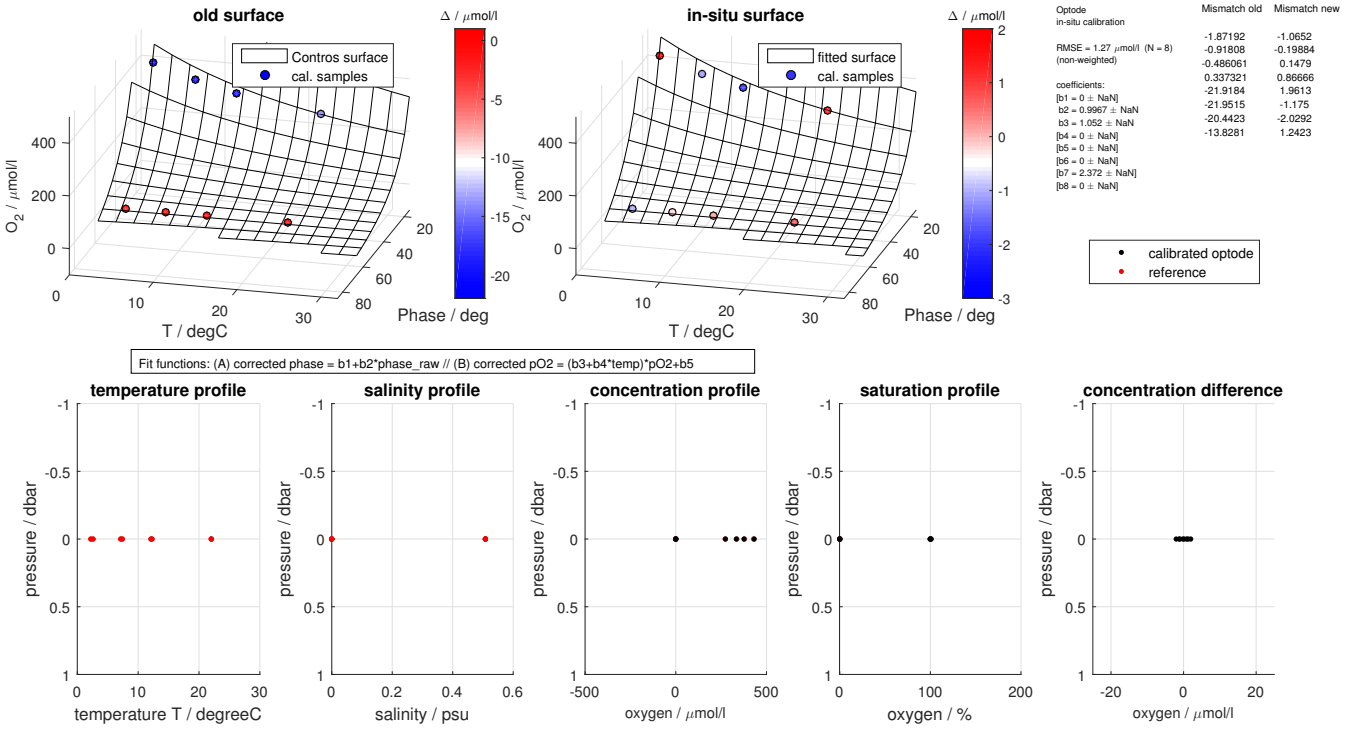

Figure S8: Re-adjustment of HF17-03 from two-point calibration 3 in the laboratory

1.2.2 Re-adjustments from field experiments

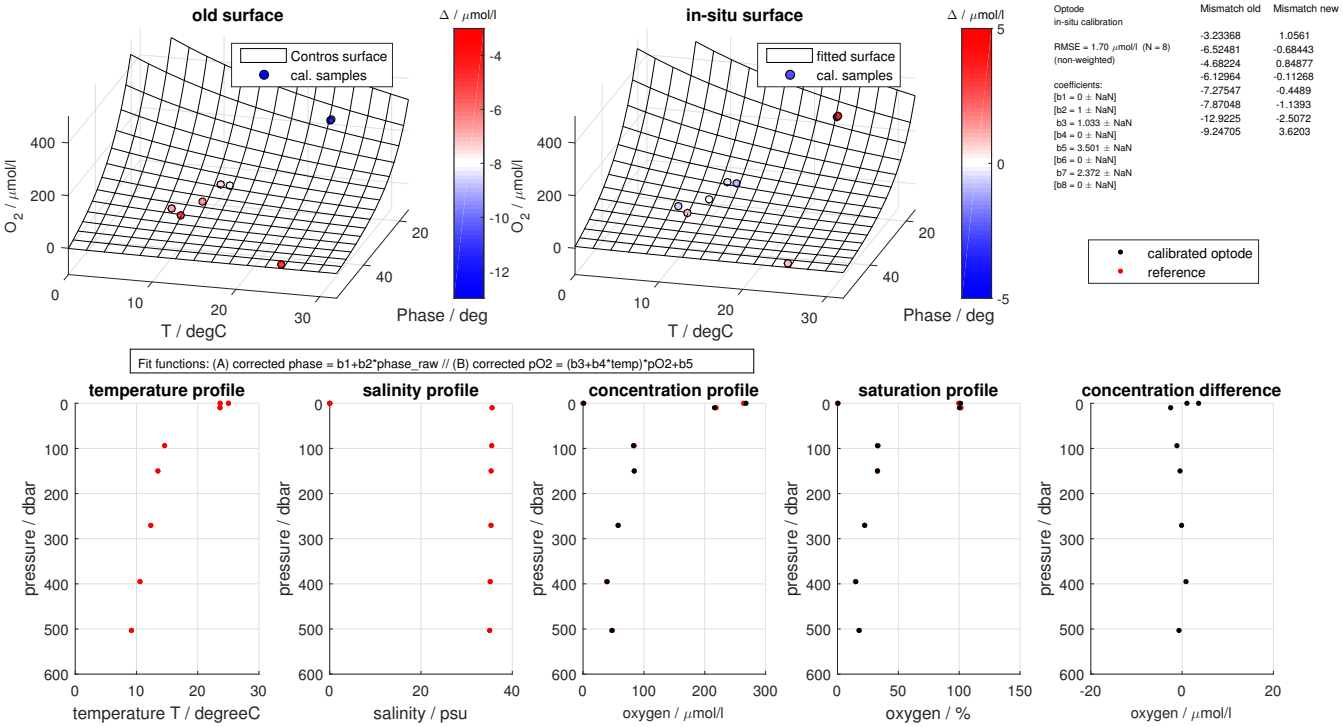

Figure S9: Re-adjustment of HF16-05 inside the original parameter space

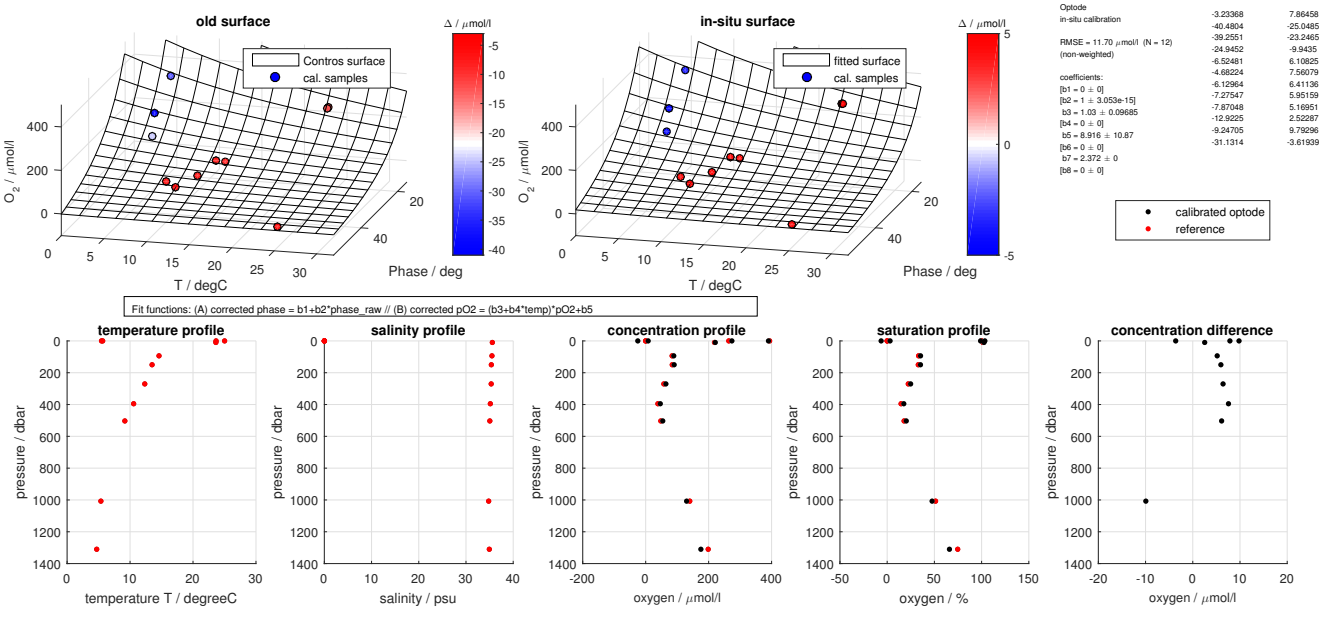

Figure S10: Re-adjustment of HF16-05 inside and outside the original parameter space

1.3 Hydrostatic pressure dependence

$$\Delta O_{2,F->0} = (a \cdot O_2(\vartheta, \varphi) + b) \cdot (1 + \frac{0.01 \cdot c \cdot p}{1000})$$

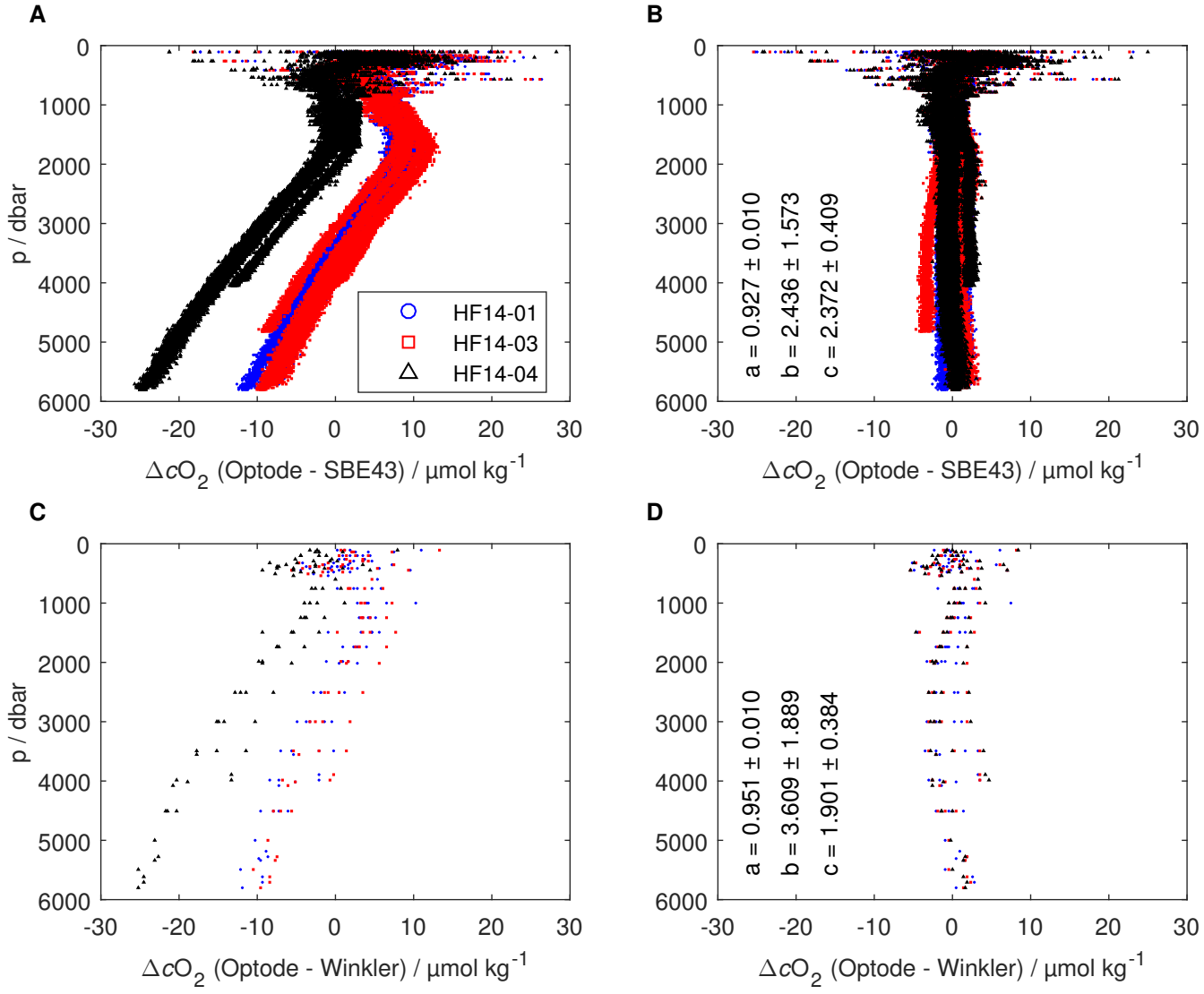

Figure S11: Results for the hydrostatic pressure dependence before (A, C) and after (B, D) applying correction Equation 6 of the CONTROS HydroFlash® O_2 optode based on SBE 43 (A, B) and Winkler (C, D) reference points. We obtained a slightly lower mean value for variable c using Winkler references samples, but yielded higher mean offsets (Optode - Winkler) taking into account all deep profiles for depths below 100 m.

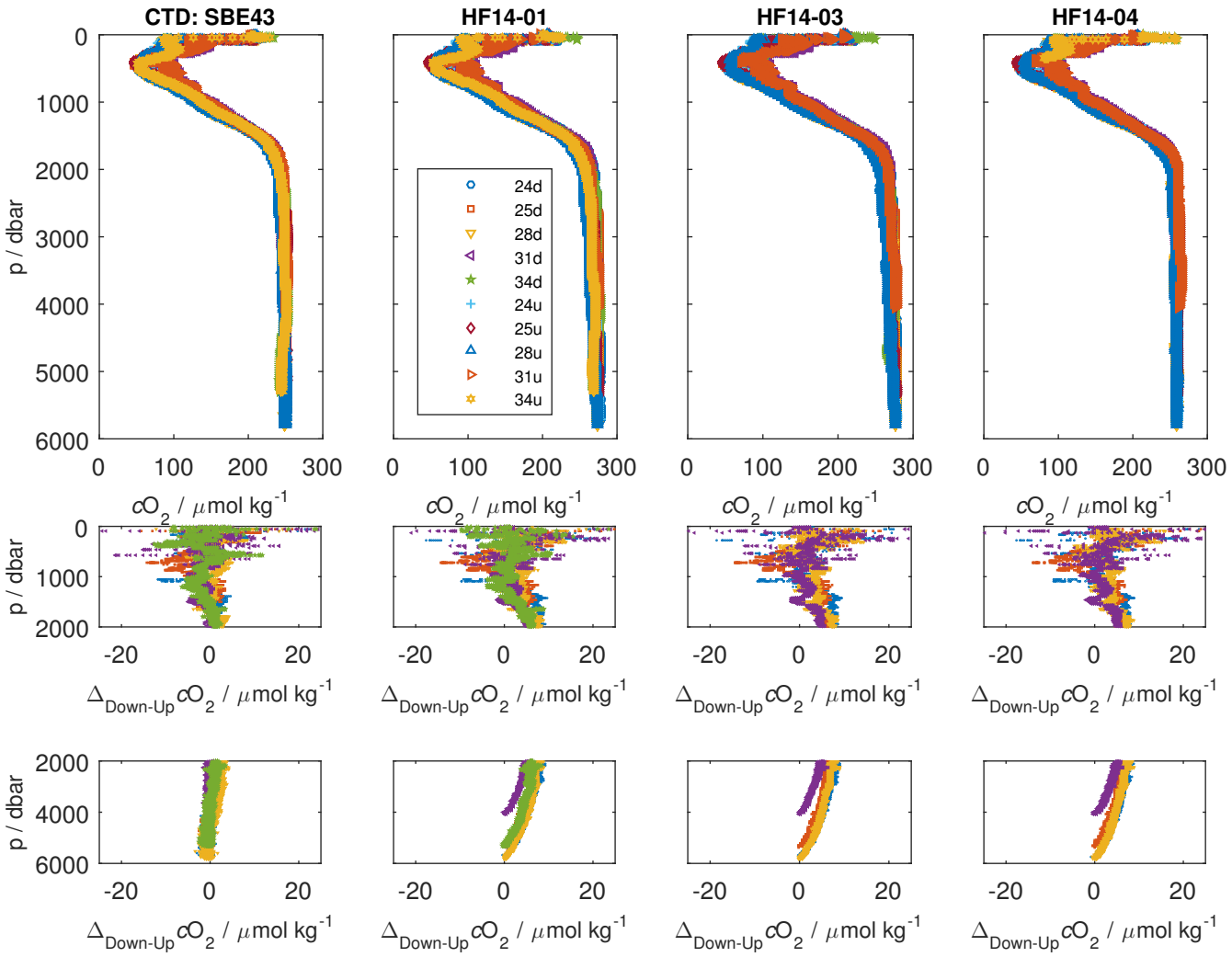

Figure S12: Potential pressure hysteresis of CONTROS HydroFlash® O_2 optodes. Given the *in-situ* character of the experiment and the unclear optode behavior in the upper 100 m, we could not fully exclude whether the optode experienced pressure hysteresis. This may be supported by the curvature of deep oxygen optode profiles (bottom row), which display the oxygen concentration difference between the downcast and the upcast.

1.4 Stability assessment

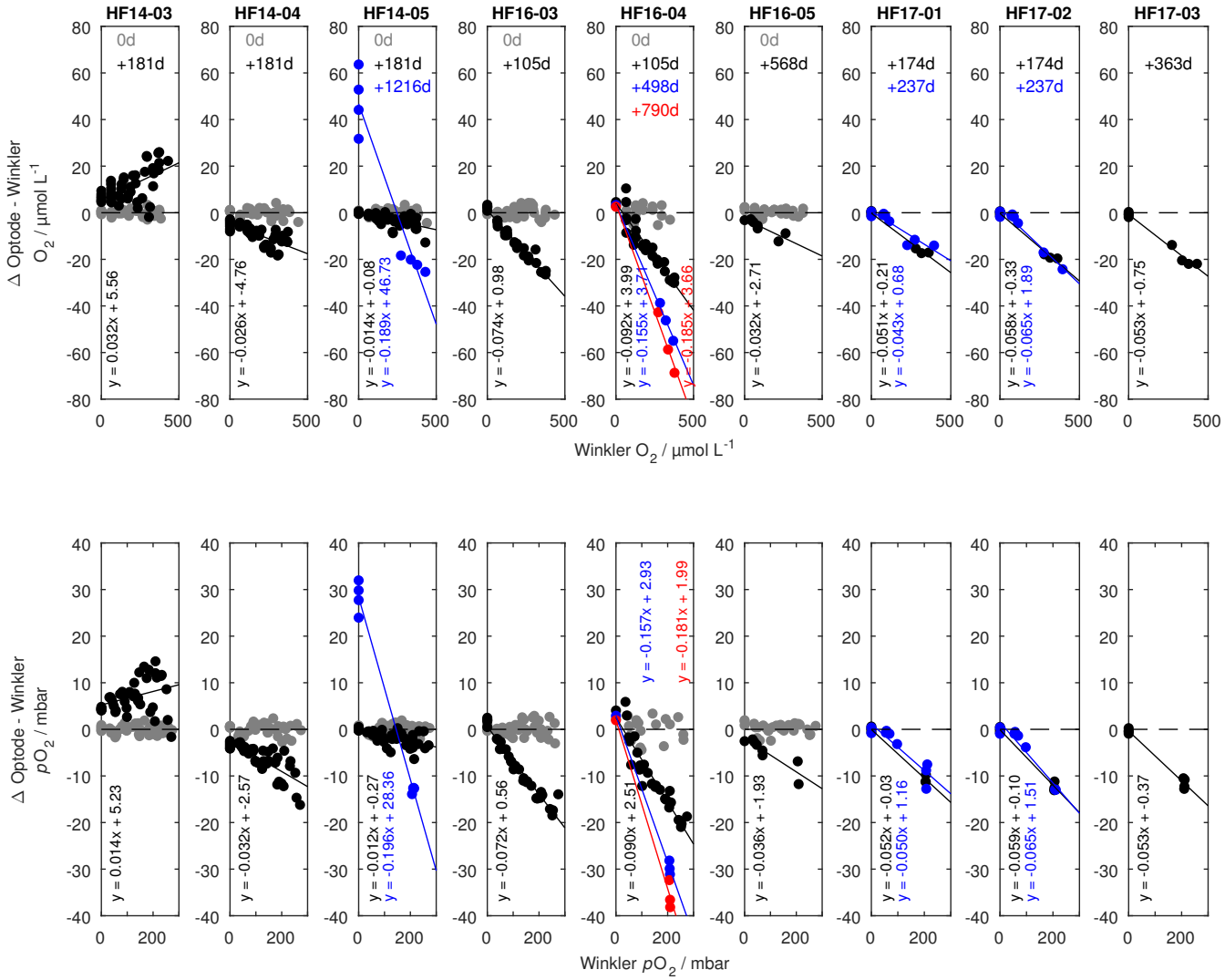

Figure S13: Drift behavior plots over time of all CONTROS HydroFlash® O_2 optodes used in this study.

1.5 Other evidences from experiments

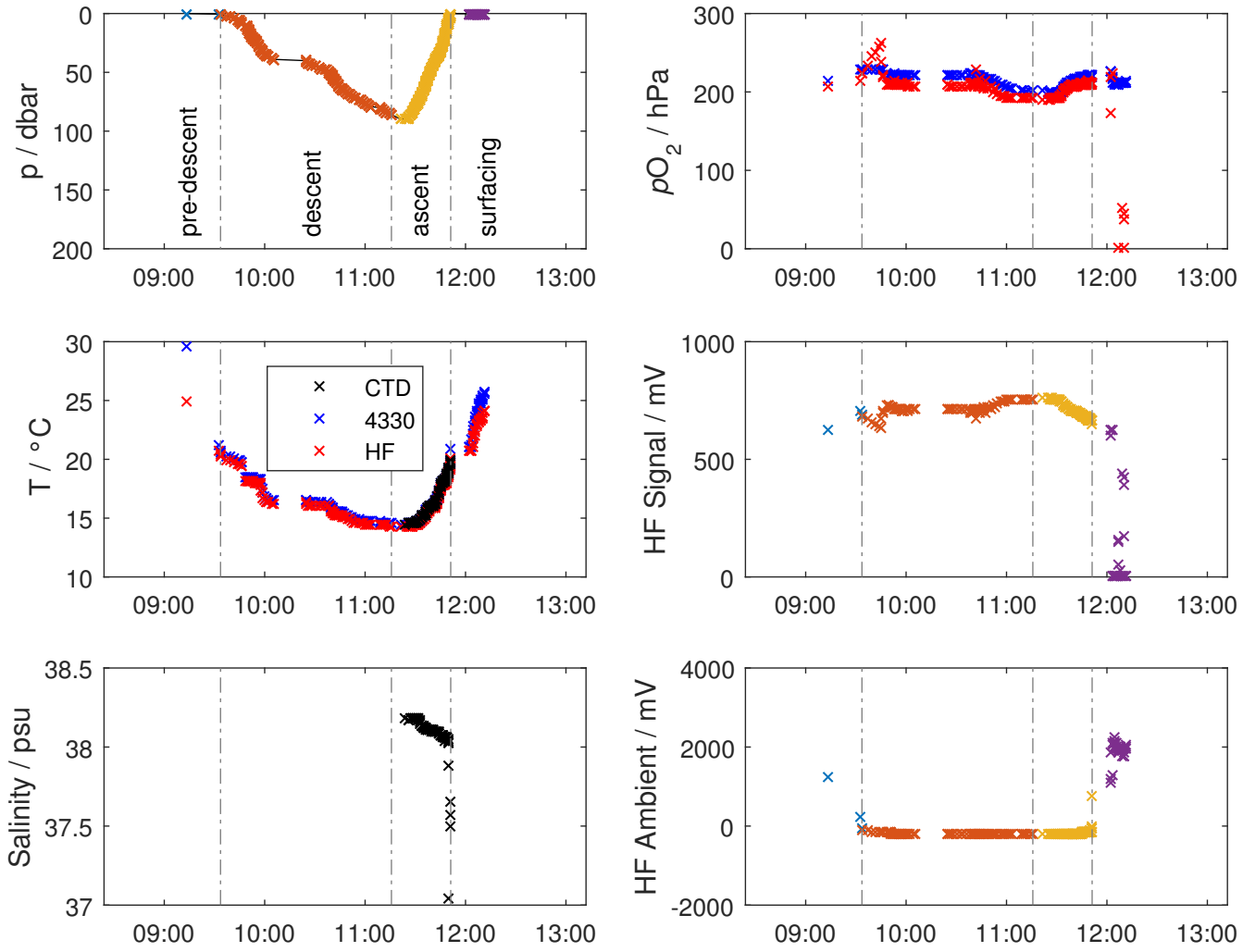

Figure S14: A proof-of-concept implementation of a CONTROS HydroFlash® O_2 optode (HF16-01) on a PROVOR Argo float in collaboration with the Laboratoire d'Océanographie de Villefranche-sur-Mer (LOV): The optode was entirely integrated in the top structure, power supply, and data string transmission of the float next to a CTD and 4330 optode, and yielded data for pressure, temperature, number of measurements, the optodes' phase shift (converted to pO_2 with temperature and calibration coefficients), signal intensity and ambient light. Data points were obtained for four different phases of the float cycle, i.e., pre-descent, descent, ascent and surfacing. While all measurements showed normal behavior before the float's full ascent, the optode revealed strong sensor spot sensitivity when exposed to direct solar irradiation at the surface at about 12:00 pm on 7th June 2016. HF16-01 obtained a multi-point calibration (MP3) about 1.5 months before the Argo float deployment, thus optode drift may explain the difference in pO_2 compared to the 4330.

2 SUPPLEMENTARY TABLES

Table S1. Properties and specifications of the latest CONTROS HydroFlash® O_2 optode (KM Contros, 2019).

Property	Description/Specifications
Housing, dimensions	Corrosion-free titanium, cylindrical, 23 mm x 170/197 mm (without/with connector)
Weight	0.17 kg in air, 0.11 kg in water
Operational depth capability	6000 m (standard)
Connector	SubConn MCBH-4M Titanium 4-pin
Supply voltage	6–32 Vdc
Power consumption	Measurement: 0.1 Ws per sample, during stand-by: 0.3 mA
Measuring principle	Dynamic luminescence quenching
Measurement range	0 – 300 mbar pO_2
Operating temperature	2 °C – 35 °C
Resolution	0.01 mbar or < 0.1 %
Initial accuracy	± 1 %
Response time ($t_{63\%}$)	$<$3 s
Sampling rate	$\leq$1 Hz (between every 1 second to 24 hours)
Wake-up time	3–4 s, if data logger is empty
Data logger	Capable of logging approx. 2 million sets of data
Data interface	RS-232C
Data format	ASCII
Battery pack	External battery pack CONTROS HydroB® Flash

Table S2. Inventory matrix of calibrated CONTROS HydroFlash® O_2 and reference optodes used in this study. The table displays several sensor versions (including our test optodes HF14-06, HF15-05 and HF15-12 which did not yield quantitative results), performance characteristics dependencies and respective field applications used over the course of this study. Legend explanation for the top column: Ox, oxygen dependence; S, salinity dependence; p, hydrostatic pressure dependence; Drift, stability assessment; τ, time dependence; UW, underway measurements in a flow-through box; CTD, profiling application on a rosette sampler in the water column; CVOO, mooring application at the Cabo Verde Ocean Observatory; Air, air measurements with strong sunlight on the top deck during M116; Float, Argo float test profile; cref, Chapter reference in the main manuscript. The symbol (x) denotes the optode facing the parameter throughout its lifetime, but not contributing substantially to the respective key sensor performance data evaluation.

Optode Letter Code	Ox	S	p	Drift	τ	UW	CTD	CVOO	Air	Float	cref
DO-1,-2,-3	-	-	-	-	x	-	-	-	-	-	3.6.1
HF14-01	x	x	x	-	-	x	x	-	x	-	3.2, 3.4, 3.6.2, 3.7
HF14-03	x	x	x	x	-	-	x	-	x	-	3.2, 3.3, 3.4, 3.5.1, 3.6.2, 3.7
HF14-04	x	x	x	x	-	-	x	-	x	-	3.2, 3.3, 3.4, 3.5.1, 3.6.2, 3.7
HF14-05	x	x	-	x	-	x	x	-	-	-	3.2, 3.3, 3.5.1
HF14-06	-	-	-	-	-	-	(x)	-	-	-	(preliminary tests)
HF15-05	-	-	-	-	-	-	-	(x)	-	-	(preliminary tests)
HF15-12	-	-	-	-	-	-	-	(x)	-	-	(preliminary tests)
HF16-01	x	(x)	-	-	-	-	-	-	-	x	3.2, 3.7
HF16-02	x		-	-	-	-	-	-	-	-	3.2
HF16-03	x	(x)	(x)	x	-	-	(x)	x	-	-	3.2, 3.5.2
HF16-04	x	(x)	(x)	x	-	-	-	-	-	-	3.2, 3.5.1
HF16-05	x	x	(x)	x	-	-	x	x	-	-	3.2, 3.3, 3.5.1, 3.5.2
HF17-01	x	-	-	x	-	-	x	x	-	-	3.2, 3.5.2
HF17-02	x	-	-	x	-	-	x	x	-	-	3.2, 3.5.2
HF17-03	x	-	-	x	-	-	-	-	-	-	3.2, 3.5.2
4330-1082	x	x	-	-	-	x	-	-	-	-	3.2, 3.3
4330-1277	x	-	-	-	-	-	-	-	-	-	3.2
4330-2238	x	-	-	-	-	-	-	-	-	-	3.2
SBE 63-392	x	-	-	-	-	-	-	-	-	-	3.2

Table S3. Mean chemical composition and ionic strength (defined as $I = \frac{1}{2}\sum_{i=1}^{n} c_\mathrm{i} \cdot z_\mathrm{i}^2$) of standard seawater (at T = 25°C, S = 35, $\rho_{\mathrm{T=25\,^\circ C}}$ = 0.997048, according to Dickson et al. (2007, chap. 5).

Species	M [$\frac{g}{mol}$]	M [$\frac{mg}{mol}$]	z_i	c [$\frac{mol}{kg_{H_2O}}$]	$c_\mathrm{i} \cdot z_\mathrm{i}^2$
Cl^-	35.453	35453	1	0.56576	0.56576
SO_4^{2-}	96.06	96060	2	0.02927	0.11708
Br^-	79.904	79904	1	0.00087	0.00087
F^-	18.998403	18998.403	1	0.00007	0.00007
Na^+	22.989769	22989.769	1	0.48616	0.48616
Mg^{2+}	24.305	24305	2	0.05475	0.219
Ca^{2+}	40.078	40078	2	0.01065	0.0426
K^+	39.0983	39098.3	1	0.01058	0.01058
Sr^{2+}	87.62	87620	2	0.00009	0.00036
$B(OH)_3$	61.83	61830	0	0.00033	0
$B(OH)_4^-$	78.84	78840	1	0.0001	0.0001
CO_2	44.01	44010	0	0.00001	0
HCO_3^-	61.0168	61016.8	1	0.00183	0.00183
CO_3^{2-}	60.008	60008	2	0.00027	0.00108
OH^-	17.008	17008	1	0.00001	0.00001
NH_4^+	17.031	17031	1	0	0
BrO_3^-	127.901	127901	1	0	0
NO_3^-	62.0049	62004.9	1	0	0
NO_2^-	46.005	46005	1	0	0
PO_4^{3-}	94.9714	94971.4	3	0	0
				$\sum$ 1.16075	
				I	0.72275
				S	35

Table S4: Chemical composition data of tab water from local municipal (Stadtwerke Kiel AG) supply locations at a) Schulensee and Schwentinetal, and b) Pries and Wik. The calculations of salinity for a) and b) result from ionic strength (defined as $I = \frac{1}{2}\sum_{i=1}^{n} c_i \cdot z_i^2$) and conductivity C of all four datasets. We used an average salinity value of S = 0.508 based on ionic strength for the final fit reference points at 100 % saturation levels during lab calibrations of CONTROS HydroFlash® O_2 optodes in this study. Note: Tab water composition data as of January 2019 was available through https://www.stadtwerke-kiel.de/swk/de/produkte/privatkunden/wasser/qualitaet/qualitaet.jsp.

a)		*Schulensee*			*Schwentinetal*	
Species	β_i [$\frac{mg}{L}$]	c [$\frac{mol}{kg_{H_2O}}$]	$c_i \cdot z_i^2$	β_i [$\frac{mg}{L}$]	c [$\frac{mol}{kg_{H_2O}}$]	$c_i \cdot z_i^2$
Cl^-	20	0.000562462	0.000562462	63	0.001771755	0.001771755
SO_4^{2-}	9	9.34149E-05	0.000373659	51	0.000529351	0.002117404
Br^-	0	0	0	0	0	0
F^-	0.19	9.97132E-06	9.97132E-06	0.21	1.10209E-05	1.10209E-05
Na^+	16.5	0.000715592	0.000715592	48.3	0.002094733	0.002094733
Mg^{2+}	10.1	0.000414326	0.001657303	11.7	0.000479961	0.001919846
Ca^{2+}	92	0.002288747	0.009154989	112	0.002786301	0.011145204
K^+	2.78	7.08929E-05	7.08929E-05	3.14	8.00733E-05	8.00733E-05
Sr^{2+}	0	0	0	0	0	0
$B(OH)_3$	0	0	0	0	0	0
$B(OH)_4^-$	0	0	0	0	0	0
CO_2	12	0.00027186	0	13	0.000294515	0
HCO_3^-	331.9	0.005423428	0.005423428	353.3	0.005773116	0.005773116
CO_3^{2-}	0	0	0	0	0	0
OH^-	0	0	0	0	0	0
NH_4^+	0.15	8.78147E-06	8.78147E-06	0.02	1.17086E-06	1.17086E-06
BrO_3^-	0.001	7.79547E-09	7.79547E-09	0.001	7.79547E-09	7.79547E-09
NO_3^-	13.9	0.000223514	0.000223514	1.92	3.08739E-05	3.08739E-05
NO_2^-	0.019	4.11779E-07	4.11779E-07	0.005	1.08363E-07	1.08363E-07
PO_4^{3-}	0.09	9.44856E-07	8.50371E-06	1	1.04984E-05	9.44856E-05
		$\sum$ 0.01008			$\sum$ 0.01386	
		I	0.00910	I		0.01252
		S	0.441	S		0.606
		$C_{T=25°C}$ [$\frac{\mu S}{cm}$]	557	$C_{T=25°C}$ [$\frac{\mu S}{cm}$]		782
		$S_{f=sal78_{SW}}$	0.270	$S_{f=sal78_{SW}}$		0.383
b)		*Pries*			*Wik*	
Cl^-	15	0.000421846	0.000421846	123	0.00345914	0.00345914
SO_4^{2-}	1.9	1.97209E-05	7.88837E-05	2.3	2.38727E-05	9.54908E-05
Br^-	0	0	0	0	0	0
F^-	0.22	1.15457E-05	1.15457E-05	0.16	8.3969E-06	8.3969E-06
Na^+	16.6	0.000719929	0.000719929	60.8	0.002636848	0.002636848
Mg^{2+}	10.2	0.000418428	0.001673712	16.3	0.000668664	0.002674657
Ca^{2+}	72	0.001791194	0.007164774	108	0.00268679	0.010747161

Table S4: (continued)

Species	β_i [$\frac{mg}{L}$]	c [$\frac{mol}{kg_{H_2O}}$]	$c_i \cdot z_i^2$	β_i [$\frac{mg}{L}$]	c [$\frac{mol}{kg_{H_2O}}$]	$c_i \cdot z_i^2$
K^+	3.02	7.70132E-05	7.70132E-05	4.96	0.000126485	0.000126485
Sr^{2+}	0	0	0	0	0	0
$B(OH)_3$	0	0	0	0	0	0
$B(OH)_4^-$	0	0	0	0	0	0
CO_2	9.1	0.000206161	0	16	0.000362481	0
HCO_3^-	283.7	0.004635814	0.004635814	366.7	0.005992079	0.005992079
CO_3^{2-}	0	0	0	0	0	0
OH^-	0	0	0	0	0	0
NH_4^+	0.079	4.62491E-06	4.62491E-06	0.0029	1.69775E-07	1.69775E-07
BrO_3^-	0.001	7.79547E-09	7.79547E-09	0.001	7.79547E-09	7.79547E-09
NO_3^-	1.36	2.1869E-05	2.1869E-05	2.58	4.14868E-05	4.14868E-05
NO_2^-	0.015	3.25089E-07	3.25089E-07	0.012	2.60071E-07	2.60071E-07
PO_4^{3-}	0.18	1.88971E-06	1.70074E-05	0.03	3.14952E-07	2.83457E-06
		$\sum$ 0.00833			$\sum$ 0.01601	
		I	0.00741		I	0.01289
		S	0.359		S	0.624
		$C_{T=25°C}$ [$\frac{\mu S}{cm}$]	462		$C_{T=25°C}$ [$\frac{\mu S}{cm}$]	902
		$S_{f=sal78_{SW}}$	0.223		$S_{f=sal78_{SW}}$	0.443
					Mean values a) & b)	
					$\bar{I}$ = 0.010±0.002	
					$\bar{S}$ = 0.508±0.112	
					$\bar{C}_{T=25°C}$ = 675.750±174.835 $\frac{\mu S}{cm}$	
					$\bar{S}_{f=sal78_{SW}}$ = 0.330±0.087	

REFERENCES

Dickson, A. G., Sabine, C. L., and Christian, J. R. (eds.) (2007). *Guide to best practices for ocean CO_2 measurements*, Sidney, British Columbia, North Pacific Marine Science Organization, 191pp. (PICES Special Publication 3; IOCCP Report 8). doi:10.25607/OBP-1342

KM Contros (2019). *CONTROS HydroFlash Datasheet*. Kongsberg Maritime Contros GmbH, Kiel, Germany.